Crosstalk analysis of silicon-on-insulator nanowire-arrayed waveguide grating*

Kai-Li Li(李凯丽), Jun-Ming An(安俊明)†, Jia-Shun Zhang(张家顺), Yue Wang(王玥), Liang-Liang Wang(王亮亮), Jian-Guang Li(李建光), Yuan-Da Wu(吴远大), Xiao-Jie Yin(尹小杰), and Xiong-Wei Hu(胡雄伟)

State Key Laboratory on Integrated Optoelectronics, Institute of Semiconductors, Chinese Academy of Sciences, Beijing 100083, *China*

(Received 22 April 2016; revised manuscript received 30 July 2016; published online 25 October 2016)

The factors influencing the crosstalk of silicon-on-insulator (SOI) nanowire arrayed waveguide grating (AWG) are analyzed using the transfer function method. The analysis shows that wider and thicker arrayed waveguides, outsider fracture of arrayed waveguide, and larger channel space, could mitigate the deterioration of crosstalk. The SOI nanowire AWGs with different arrayed waveguide widths are fabricated by using deep ultraviolet lithography (DUV) and inductively coupled plasma etching (ICP) technology. The measurement results show that the crosstalk performance is improved by about 7 dB through adopting 800 nm arrayed waveguide width.

Keywords: SOI, nanowire AWG, crosstalk, phase errors

PACS: 42.79.Sz, 42.82.Bq, 42.82.Et **DOI:** 10.1088/1674-1056/25/12/124209

1. Introduction

In the past few decades, the rapid growth of large capacity data service has dramatically promoted the development of optical networks. Among the different kinds of optical components in optical networks, silicon photonics is promising due to its advantages of low cost, high stability and compatibility with complementary metal oxide semiconductor (CMOS) processing technology.[1] In recent years, many devices based on SOI have been demonstrated.[2–5] Among them, the arrayed waveguide grating (AWG) is a key unit in silicon photonics integrated components for wavelength multiplexing or demultiplexing. Many studies based on SOI nanowire AWGs have been reported.[6–8]

The nanowire waveguides used in SOI nanowire AWG have high refractive indices, giving rise to strong modal confinement and very small bend radius.[9,10] This results in the fact that the SOI nanowire AWGs can be minimized to a size on the order of μm^2. However, it induces a very high sensitivity to fabrication tolerance, making it difficult to reduce the crosstalk of SOI nanowire AWG.[11] The methods of restraining crosstalk like a smaller mask grid,[12] parabolic tapers,[13] bi-level taper and broadening arrayed waveguide width[14] have been proposed, but there are no analyses in detail about the influences on crosstalk.

In this paper, according to the transfer function method, we analyze the factors influencing the crosstalk, such as width variations, thickness variations, fracture of arrayed waveguides and channel spacing. The experimental results demonstrate that it is an effective method to reduce crosstalk by broadening the arrayed waveguide width.

2. Analysis and simulation

An SOI nanowire AWG is composed of input/output waveguides, arrayed waveguides and input/output slab waveguides as shown in Fig. 1. The length difference and effective refractive index of adjacent arrayed waveguides are ΔL and n_c, respectively. The fluctuations of n_c and ΔL will deteriorate the crosstalk of SOI nanowire AWGs. In order to analyze this influence, the spectral response can be expressed as a simple transfer function[15] on the assumption that the light input into and output from its center input and output ports, are expressed, respectively, as

$$T = \left| \sum_{j=-M}^{M} \rho_g(j,0) \times \exp \mathrm{i} \frac{2\pi}{\lambda} [j(n_{cj} \times \Delta L_j + \mathrm{rad}(a(j)))] \right|^2, \quad (1)$$

$$\mathrm{Loss(dB)} = 10 \times \log_{10} T, \quad (2)$$

where M is half the number of arrayed waveguides, $\rho_g(j,0)$ is the Gaussian mode field distribution of the j-th arrayed waveguide, $\mathrm{rad}(a(j))$ is the random fluctuation of $n_{cj} \times \Delta L$ and it deteriorates the crosstalk performance. Here, the random fluctuation of n_{cj}, caused by the width or thickness fluctuations of the j-th arrayed waveguides, are considered, equation (1) can be simplified into

$$T = \left| \sum_{j=-M}^{M} \rho_g(j,0) \times \exp \mathrm{i} \frac{2\pi}{\lambda} [j(n_{cj} + \mathrm{rad}(n_{cj})) \times \Delta L_j] \right|^2. \quad (3)$$

*Project supported by the National High Technology Research and Development Program of China (Grant No. 2015AA016902), the National Natural Science Foundation of China (Grant Nos. 61274047, 61435013, 61307034, and 61405188), and the National Key Research and Development Program of China (Grant No. 2016YFB0402504).

†Corresponding author. E-mail: junming@semi.ac.cn

© 2016 Chinese Physical Society and IOP Publishing Ltd

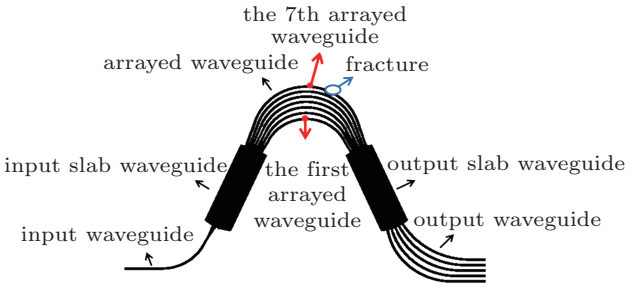


Fig. 1. (color online) Schematic diagram of an SOI nanowire AWG.

2.1. Crosstalk analysis for AWG with width fluctuation of waveguide

An SOI wafer with a 220-nm thick top silicon layer on a 2-μm thick buried oxide layer is used for the AWG simulation. Using Eq. (3), we analyze the effects of width fluctuation on the crosstalk of SOI nanowire AWG, where the design parameters of SOI nanowire AWGs are listed in Table 1 according to the diffraction equation of AWGs.

Table 1. AWG design parameters.

Parameters	AWG (#1)	AWG (#2)
Waveguide width/μm	0.5	0.8
Channel spacing/nm	1.6	1.6
The effective index of slab waveguide	2.847397	2.847397
The effective index of arrayed waveguide n_c	2.444148	2.68344541
Number of I/O channels	8	8
Radius of Rowland circle/μm	44.1056	77.4947
Difference of arrayed waveguides ΔL/μm	23.4945	30.6531
Number of arrayed waveguides	39	39

The width fluctuation ΔW of arrayed waveguide can be introduced in the etching process. We simulate this phenomenon by the normrnd function in MATLAB, the ΔW average value is zero, the standard deviation is 0.001 and it corresponds to about ±2 nm width fluctuation of arrayed waveguide. The width fluctuation ΔW results in the fluctuation of n_c as shown in Eq. (3). To increase the reliability of the simulated results, we repeat it 5 times under the conditions of the same width fluctuations and choose the maximum of crosstalk. Figure 2 shows the relationship between crosstalk and arrayed waveguide width with the same fluctuation values. From this figure, we can see that the crosstalk decreases with the increase of waveguide width. This means that a wider width of arrayed waveguide with the same fluctuation values can restrain the crosstalk.

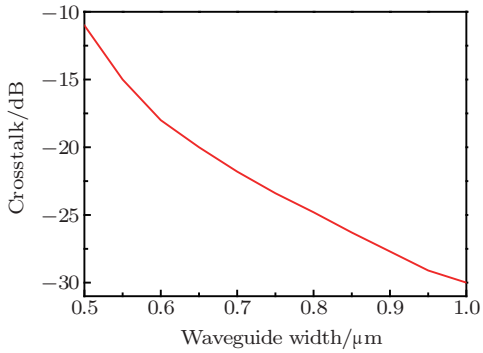


Fig. 2. (color online) Simulated results of crosstalk for AWGs with different waveguide widths.

To further analyze the influences of width fluctuations on crosstalk, simulated spectra of SOI AWGs are shown in Figs. 3(a) and 3(b), and the corresponding arrayed waveguide widths are 0.5 μm and 0.8 μm, respectively. The red curves represent the spectral responses without width fluctuations, while the other five curves refer to the spectral responses with random width fluctuations. As shown in Figs. 3(a) and 3(b), the crosstalk is about −65 dB in the ideal condition. Because of the width fluctuations, crosstalks increase to −11 dB and −25 dB for 0.5-μm and 0.8-μm widths of the arrayed waveguide, respectively.

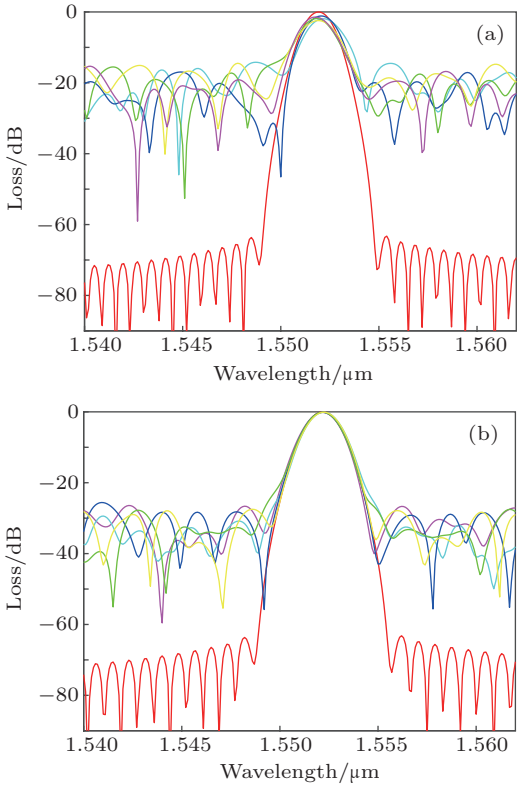


Fig. 3. (color online) Simulated spectra of SOI nanowire AWGs. (a) Arrayed waveguide width is 0.5 μm. (b) Arrayed waveguide width is 0.8 μm.

The effective index n_c, as a function of the waveguide width, is calculated using the film mode matching method, and the results are shown in Fig. 4(a). It can be seen that the slope coefficient dn_c/dW decreases with the increase of arrayed waveguide width. The values are 1.3756/μm and 0.359/μm at 0.5-μm and 0.8-μm width of arrayed waveguide, respectively. That means that the crosstalk of SOI nanowire AWGs with a wider arrayed waveguide width are less sensitive to waveguide width fluctuations in the fabrication progress. We infer that broadening the waveguide width is beneficial to reducing the crosstalk, which is in agreement with the reported results in Ref. [16].

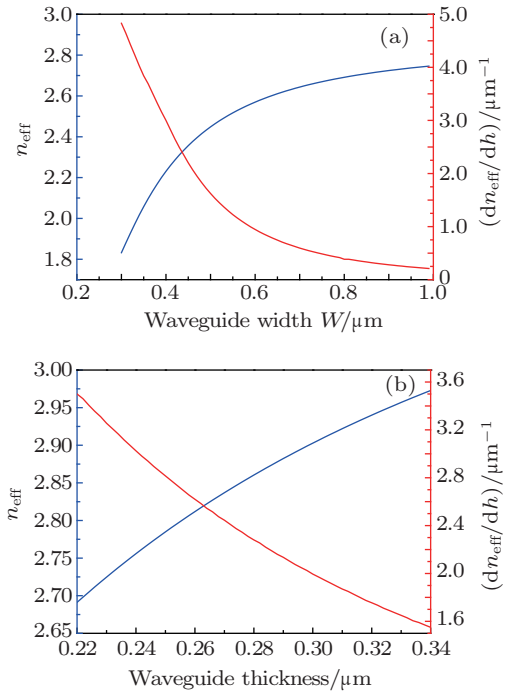


Fig. 4. (color online) Dependences of waveguide effective index on (a) waveguide width and (b) waveguide thickness.

2.2. Crosstalk analysis for AWG with thickness fluctuation of waveguide

The fluctuation of SOI wafer thickness is inevitable during wafer deposition, which will affect the crosstalk of SOI nanowire AWG. At 0.5-μm and 0.8-μm widths of arrayed waveguide, the relationships between crosstalk and arrayed waveguide thickness at the same fluctuation values Δh are shown in Fig. 5. The values of fluctuation Δh of arrayed waveguide thickness are introduced using the same method as that in Subsection 2.1, the standard deviation of Δh is 0.001 corresponding to ±2 nm of the thickness fluctuation of arrayed waveguide. We also conduct the simulation 5 times to guarantee the dependability. As can be seen in this figure, as waveguide thickness increases, the crosstalk gradually decreases. This indicates that SOI nanowire AWG with a thicker thickness of arrayed waveguide has better crosstalk performances.

Figures 6(a) and 6(b) show the simulated spectra of SOI AWGs with 220-nm and 340-nm waveguide thickness, respectively. The crosstalk is about −65 dB when there is no thickness fluctuation as shown in the red curves. As the thickness fluctuation is introduced, the crosstalks of SOI nanowire AWGs soar to −3 dB and −14 dB for 220-nm and 340-nm thickness of arrayed waveguide, respectively, as shown in the other five curves. Compared with that in Subsection 2.1, the crosstalk is very sensitive at the same ±2-nm thickness fluctuations of arrayed waveguides.

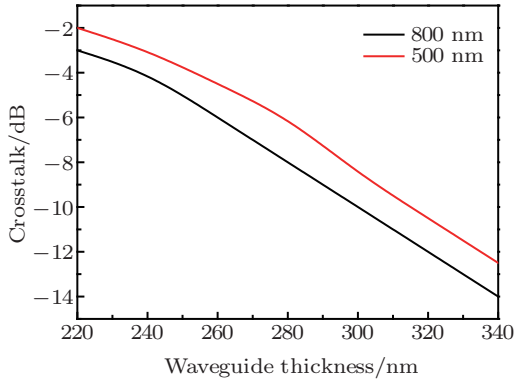


Fig. 5. (color online) Simulated results of crosstalk for AWGs with different waveguide thickness.

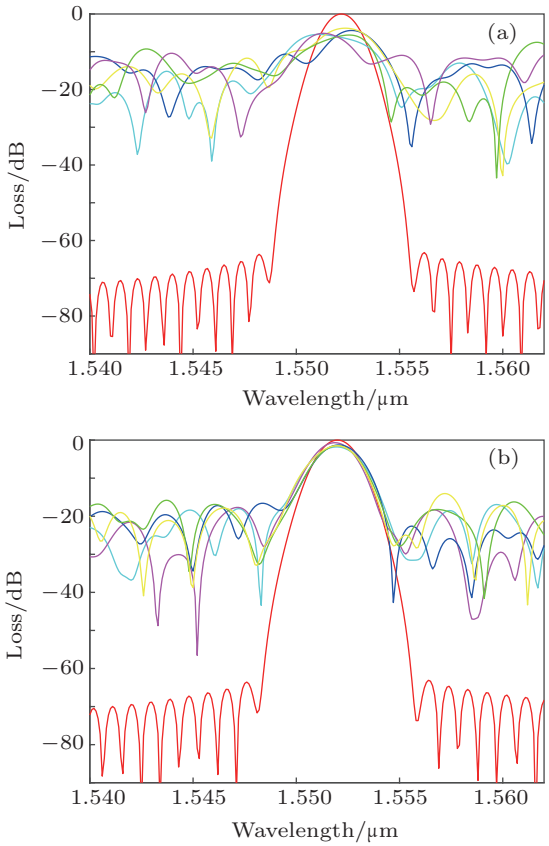


Fig. 6. (color online) Simulated spectra of SOI nanowire AWGs. (a) Arrayed waveguide thickness is 220 nm. (b) Arrayed waveguide thickness is 340 nm.

Figure 4(b) shows the relationship between the effective index n_c and the waveguide thickness. It can be seen that n_c increases with the increase of waveguide thickness, while the slope coefficient dn_c/dh decreases. That means that

the crosstalk can be improved by selecting SOI wafer with a thicker top silicon layer.

2.3. Crosstalk analysis for AWG with waveguide fracture

In the fabrication process, the fracture of the arrayed waveguides may occur as shown in Fig. 1. The fracture of the arrayed waveguide at different positions will result in different levels of influence on crosstalk. Figure 7(a) shows the relationship between crosstalk and waveguide fracture position. Figure 7(b) shows the simulated spectra of SOI AWGs with the waveguide fracture in the 1st, 7th, 19th, and 25th arrayed waveguides, respectively. It can be seen that the waveguide fracture on the outside has less influence on crosstalk. As the fracture position varies from the marginal arrayed waveguide to the central arrayed waveguide, the crosstalk increases and reaches a maximum of −22.5 dB at a fracture position of the 20th arrayed waveguide. That is because the propagating power is of a Gaussian profile, the power in the central waveguide is maximal. The fracture in the central arrayed waveguide will lead to a large optical power loss and poor crosstalk performance.

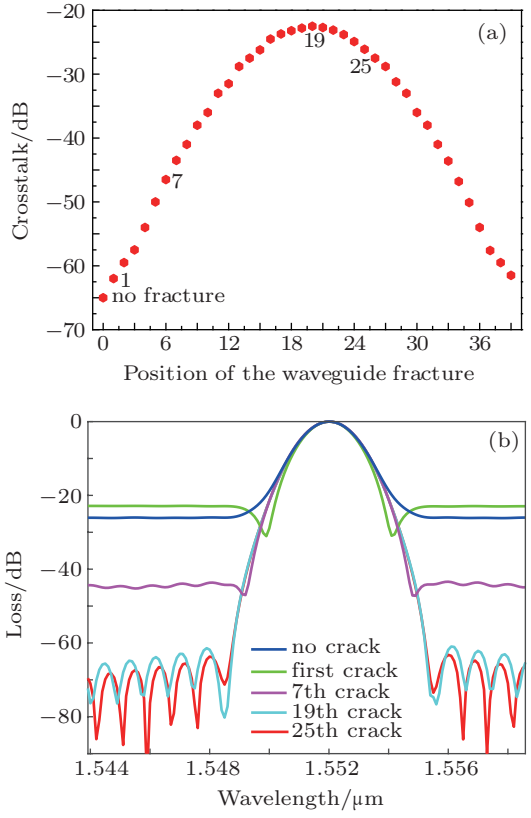


Fig. 7. (color online) (a) Relationship between crosstalk and waveguide fracture positions. (b) Simulated spectra of SOI nanowire AWGs at different waveguide fracture positions.

2.4. Crosstalk analysis for AWG with different channel spacings

When the width of arrayed waveguide is 0.8 μm, we further discuss the effects of width fluctuations on crosstalk for SOI nanowire AWGs with different channel spacings as shown in Fig. 8. From Fig. 8, we can see that the crosstalk decreases with the increase of channel spacing. Figures 9(a) and 9(b) show the simulated spectra of the SOI nanowire AWGs with channel spacings of 0.8 nm and 6.4 nm, respectively. The corresponding crosstalks of AWGs with width fluctuations are −21.5 dB and −34 dB respectively. The reason is that the influence on crosstalk is determined by the fluctuation of n_c multiplied by ΔL. The larger the channel spacing, the smaller the value of ΔL is, and the fluctuation of n_c multiplied by ΔL is smaller. So, the corresponding phase errors decrease and, as a result, the crosstalk will be reduced accordingly. We can infer that SOI nanowire AWG is more suitable for coarse wavelength division multiplexing (CWDM) application.

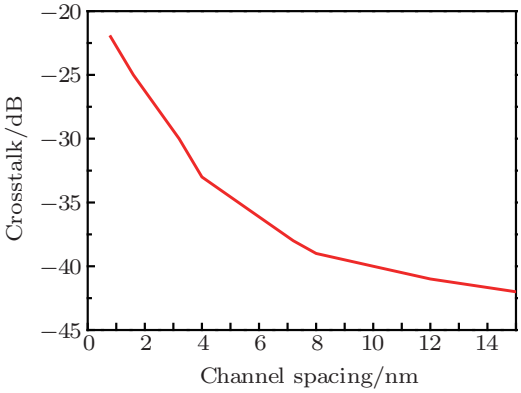


Fig. 8. (color online) Simulated results of crosstalk for AWGs with different channel spacings.

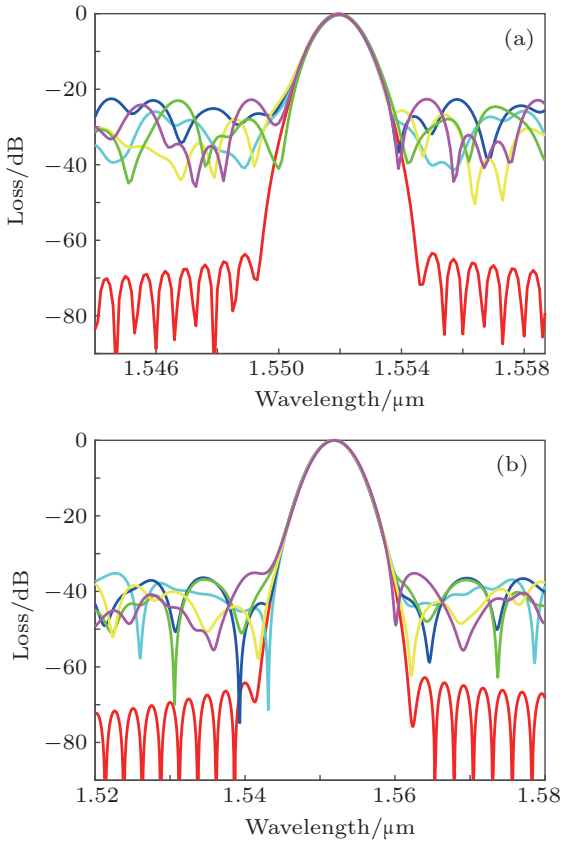


Fig. 9. (color online) Simulated spectra of SOI nanowire AWG. (a) Channel spacing is 0.8 nm. (b) Channel spacing is 6.4 nm.

3. Fabrication and measurement

Based on the above analysis, the SOI nanowire AWGs of 0.5-μm and 0.8-μm arrayed waveguide widths are fabricated with DUV and ICP technology. The basic parameters of the AWG are consistent with the parameters in Table 1. Each the devices is based on the wafer with a 220-nm-thick top silicon layer and a 2-μm-thick buried oxide layer. The microscope pictures of the fabricated AWGs are shown in Fig. 10. AWG (#1) and AWG (#2) correspond to 0.5-μm and 0.8-μm waveguide widths, respectively, where the broadening waveguide width of AWG (#2) is only at the section of straight arrayed waveguide to ensure less bend loss.

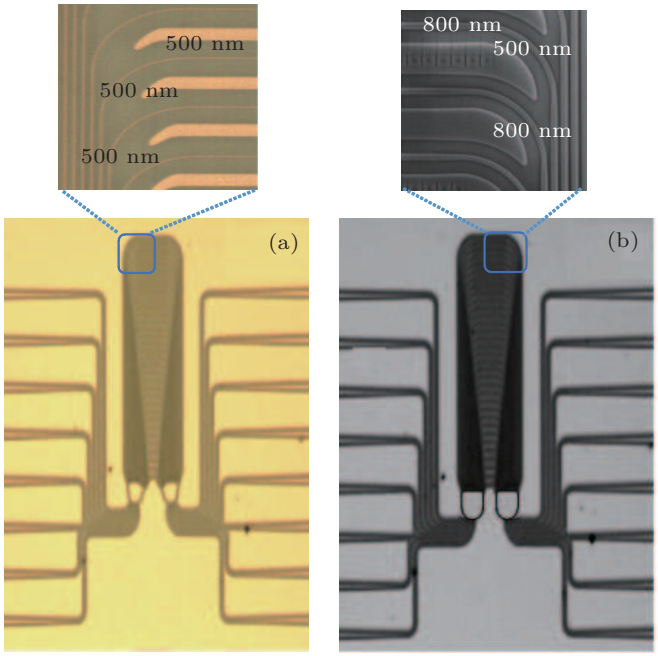


Fig. 10. (color online) Microscope pictures of SOI nanowire (a) AWG (#1) and (b) AWG (#2). Insets: the detail views of the bends in the arrayed waveguide.

The characteristics of the AWGs are measured by using an amplified spontaneous emission (ASE), a polarization controller, fiber alignment stages, and an optical spectrum analyzer (Yokogawa AQ6370B). After performing chip dicing and facet polishing, an ASE with a spectrum range of 1520 nm–1600 nm through a polarization controller is coupled into the input waveguide of AWG, and then detected in the output ports with a spectrum analyzer, by moving the output fiber from one channel to the next after each wavelength scan.

The measured spectra of AWG (#1) and AWG (#2) are shown in Figs. 11(a) and 11(b) respectively. It can be seen that the central wavelengths are deviated from the design values due to fabrication errors, the crosstalks of AWG (#1) and AWG (#2) are about −8 dB and −15 dB, respectively. The fluctuation of arrayed waveguide results in the fluctuations of n_c, thus degrading the imaging quality of the output waveguide. By broadening the waveguide width, the crosstalk is obviously improved. According to the discussion above, it can be proved that it is effective to restrain the crosstalk by broadening the waveguide width, which is consistent with the reported results in Ref. [16].

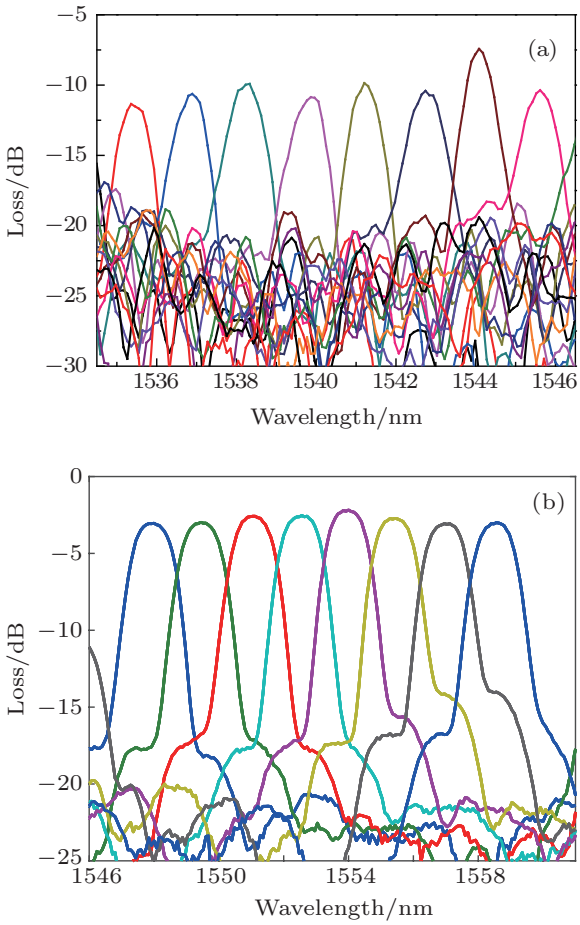


Fig. 11. (color online) Measured spectra of SOI nanowire (a) AWG (#1) and (b) AWG (#2).

4. Conclusions

In this paper, the crosstalk of SOI nanowire AWG is analyzed theoretically and experimentally. The factors influencing the crosstalk are investigated in detail by using the transfer function method. The theoretical results indicate that wider and thicker arrayed waveguides, outsider fracture of arrayed waveguide, and larger channel spacing could mitigate the deterioration of crosstalk. AWGs with different arrayed waveguide widths are fabricated. The experimental results show that SOI nanowire AWG has a crosstalk improvement of 7 dB by broadening the arrayed waveguide width.

References

[1] Bogaerts W, Baets R, Dumon P, Wiaux V, Beckx S, Taillaert D, Luyssaert B, Van Campenhout J, Bienstman P and Van Thourhout D 2005 *J. Lightwave Technol.* **23** 401

[2] Xie B Q, Li B, Bi J S, Bu J H, Wu C, Li B H, Han Z S and Luo J J 2016 *Chin. Phys. B* **25** 078501

[3] Wu W K, An X, Jiang X B, Chen Y H, Liu J J, Zhang X and Huang R 2015 *J. Semicond.* **36** 114001

[4] An J M, Wu Y D, Li J, Li J G, Wang H J, Li J Y and Hu X W 2008 *Chin. Phys. Lett.* **25** 1717
[5] Wu W K, An X, Tan F, Feng H, Chen Y H, Liu J J, Zhang X and Huang R 2015 *J. Semicond.* **36** 114004
[6] Fang Q, Liow T Y, Song J F, Ang K W, Yu M B, Lo G Q and Kwong D L 2010 *Opt. Express* **18** 5106
[7] Bogaerts W, Selvaraja S K, Dumon P, Brouckaert J, De Vos K, Thourhout D V and Baets R 2010 *IEEE J. Select. Top. Quantum Electron.* **16** 33
[8] Yuan P, Wu Y D, Wang Y, An J M and Hu X W 2015 *J. Semicond.* **36** 084005
[9] Bogaerts W, Dumon P, Thourhout D V, Taillaert D, Jaenen P, Wouters J, Beckx S, Wiaux V and Baets R G 2006 *IEEE J. Select. Top. Quantum Electron.* **12** 1394
[10] Pathak S, Lambert E, Dumon P, Thourhout D V and Bogaerts W 2011 *Proceedings of the 8th IEEE International Conference on Group IV Photonics*, September 14–16, 2011, England, London, pp. 45–47
[11] Selvaraja S K, Bogaerts W, Dumon P, Thourhout D V and Baets R 2010 *IEEE J. Select. Top. Quantum Electron.* **16** 316
[12] Pathak S, Vanslembrouck M, Dumon P, Thourhout D V, Verheyen P, Lepage G, Absil P and Bogaerts W 2014 *IEEE Photon. Technol. Lett.* **26** 718
[13] Ye T, Fu Y F, Qiao L and Chu T 2014 *Opt. Express* **22** 31899
[14] Wang J, Sheng Z, Li L, Albert P, Wu A M, Li W, Wang X, Zou Sh Ch, Qi M H and Gan F W 2014 *Opt. Express* **22** 9395
[15] Adar R, Henry C H and Dragone C 1993 *J. Lightwave Technol.* **11** 212
[16] Pathak S, Vanslembrouck M, Dumon P, Thourhout D V and Bogaerts W 2012 *Opt. Express* **20** B493